JPG Journal of Petroleum Geology www.jpg.co.uk

OIL CHARGE HISTORY OF BITUMENS OF DIFFERING MATURITIES IN EXHUMED PALAEOZOIC RESERVOIR ROCKS AT TIANJINGSHAN, NW SICHUAN BASIN, SOUTHERN CHINA

Q. Zhou[1,3], X.M. Xiao[1*], H. Tian[1] and R.W.T. Wilkins[2]

Low-maturity soft bitumen (or biodegraded heavy oil) and higher maturity solid bitumen are present in Palaeozoic siliciclastics at Tianjingshan in the NW Sichuan Basin, southern China. The origin of these bitumens of variable maturities was investigated. Samples of low-maturity bitumen from Lower Devonian sandstones and high- and low-maturity bitumen from Upper Cambrian siltstones were analysed to investigate their organic geochemistry and stable isotope compositions. Lower Cambrian and Upper Permian black shales were also investigated to assess their source rock potential, and the burial and maturation history of potential source rocks was modelled using PetroMod. Liquid and gaseous hydrocarbon fluid inclusions in the Devonian sandstones were analysed.

Results suggest that both the soft and solid bitumens are derived from crude oil generated by Lower Cambrian organic-rich black shales. Reservoir rocks at Tianjingshan have experienced two separate oil charge events – in the early-middle Triassic and early-middle Jurassic, respectively. The first oil charge was generated by Lower Cambrian black shales in a kitchen area located in the hanging wall of the Tianjingshan fault. The later oil charge was also derived from Lower Cambrian black shales, but the kitchen area was located in the footwall of the fault. Movement on the Tianjingshan fault resulted in progressive burial of the Lower Devonian sandstone reservoir rocks until the end of the middle Triassic, and the "early" charged oil was thermally degraded into high-maturity solid bitumen. The later-charged oil was altered into soft bitumen of lower maturiy by biodegradation during uplift of the reservoir after the Jurassic.

INTRODUCTION

Solid bitumen interpreted as thermally-degraded crude oil has been reported in Lower Palaeozoic to Mesozoic reservoir rocks in the Sichuan Basin and other areas in southern China (Fig. 1). The bitumen is generally encountered at depths of 3000-6000 m and accumulations discovered include *Gaoshiti* in the centre of the Sichuan Basin (Wang *et al*., 1997; Zhang *et al*., 2005; Xiao *et al*., 2007), *Weiyuan* and *Ziyang* in the south (Sun *et al*., 2007; Liu *et al*., 2008, 2009; Huang *et al*., 2011), and *Feixianguan* in the NE of the basin (Xie *et al*., 2005; Zhao *et al*., 2006; Qin *et al*., 2007; Wang *et al*., 2008; Zhao *et al*., 2012).

[1] State Key Laboratory of Organic Geochemistry, Guangzhou Institute of Geochemistry, Chinese Academy of Sciences, Guangzhou 510640, China.
[2] CSIRO Earth Science and Resource Engineering, PO Box 136, North Ryde, NSW, Australia.
[3] University of Chinese Academy of Sciences, Beijing 100049, China.
* corresponding author, email: xmxiao@gig.ac.cn

Key words: Sichuan Basin, China, Tianjingshan anticline, Lower Devonian, Cambrian, sandstones, bitumen, black shales, oil charge, fluid inclusions.

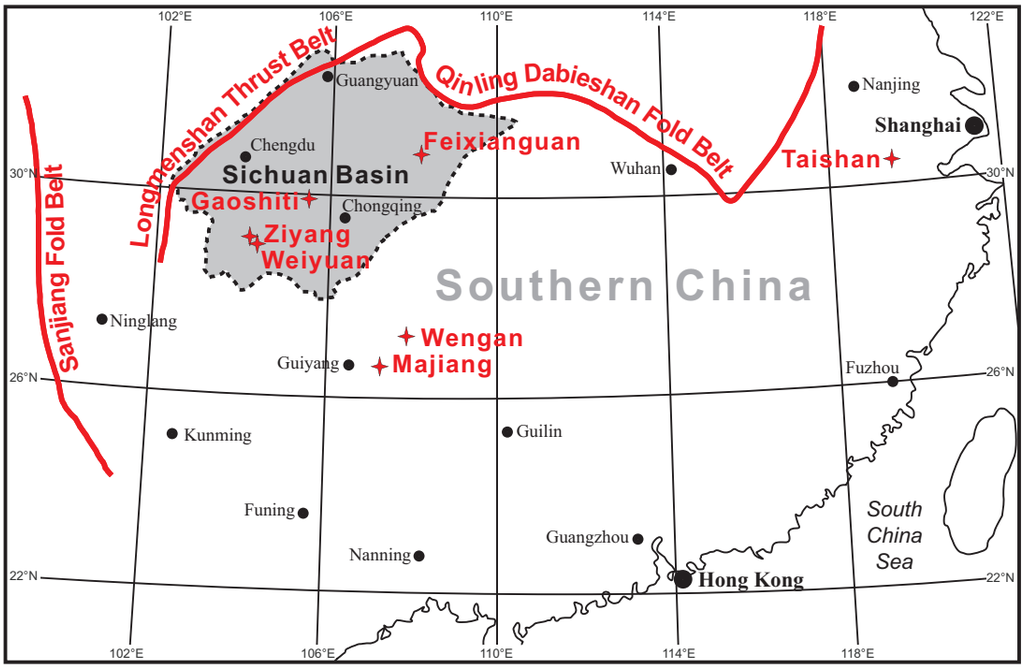

Fig. 1. Regional map of southern China showing the location of the Sichuan Basin and of exhumed palaeo -oil accumulations (red crosses).

Bitumen is also present at the surface in exhumed reservoirs such as *Majiang* and *Wengan* in Guizhou Province and *Taishan* in Zhejiang Province (Han *et al*., 1982; Liu *et al*., 1985; Wang *et al*., 1997; Xiang *et al*., 2008; Gao *et al*., 2009; Lin *et al*., 2011; Niu *et al*., 2011). These accumulations are of different sizes with reserves ranging from 0.13 to 32.2 × 10^9 brl (Wang *et al*., 1997; Sun *et al*., 2007; Xiang *et al*., 2008; Huang *et al*., 2011). The ages of the reservoir rocks range from Late Ediacaran to Early Triassic (Han *et al*., 1982; Wang *et al*., 1997; Xie *et al*., 2005; Zhang *et al*., 2005; Liu *et al*., 2008, 2009).

The bitumen is interpreted to be derived from crude oils which have undergone intense thermal degradation (Xie *et al*., 2005; Sun *et al*., 2007; Xiao *et al*., 2007; Wang *et al*., 2008; Zhao *et al*., 2012). Co-generated natural gas occurs in commercial accumulations such as the *Puguang* field in the NE Sichuan Basin (Ma *et al*., 2008). However in most cases the gas has been lost because trap structures have been destroyed (Wang *et al*., 1997).

Regional petroleum geological observations indicate that the bitumen is probably derived from oil generated by Lower Cambrian and/or Lower Silurian marine black shales (Wang *et al*., 1997; Huang *et al*., 2011; Lin *et al*., 2011). Palaeozoic reservoir rocks in southern China have generally reached very high thermal maturities. Equivalent VR_o (vitrinite reflectance) values are 2-4% for the Lower Palaeozoic (Xiao *et al*., 2007; Zhang *et al*., 2008; Liu *et al*., 2009) and 1.5-2.5% for the Upper Palaeozoic and Lower Triassic (Xiao *et al*., 2007; Wang *et al*., 2008; Zhao *et al*., 2012). It is therefore unlikely that liquid petroleum will be preserved in these reservoir units to the present day if it has experienced the same maximum palaeo-temperatures as the host reservoir rocks.

An exhumed bitumen accumulation has recently been discovered in the NE part of the Longmenshan fold-thrust belt in the NW Sichuan Basin (Fig. 2a, b) (Liu *et al*., 2003; Zhou *et al*., 2007; Deng *et al*., 2008; Liu *et al*., 2010), in a hangingwall anticline associated with the Tianjingshan fault (the Tianjingshan anticline: Fig. 2c, d). Devonian and Carboniferous strata occur at the core of the anticline whose flanks consist of a Permian, Triassic and Jurassic succession (Fig. 2d). Abundant low-maturity bitumen is present here at outcrop in exhumed Lower Devonian sandstones. The bitumen is in fact more correctly referred to as a heavy oil because it is very soft and can be completely dissolved in dichloromethane. About 400 × 10^6 brl of bitumen is estimated to be present here but the accumulation has not been commercially developed.

In addition to this low-maturity bitumen, high-maturity solid bitumen occurs in Lower Devonian sandstones in the Tianjingshan anticline (Liu *et al*., 2003); similar solid bitumen is also present in Upper Cambrian siltstones in the Kuangshanliang area to the NE of the anticline (Fig. 2b) (Liu *et al*., 2003; Zhou *et al*., 2007).

Previous studies have investigated the sedimentary characteristics of the reservoir rocks at Tianjingshan (Zhou *et al*., 2007; Deng *et al*., 2008) and the source of the bitumen (Huang and Wang, 2008; Rao *et al*.,

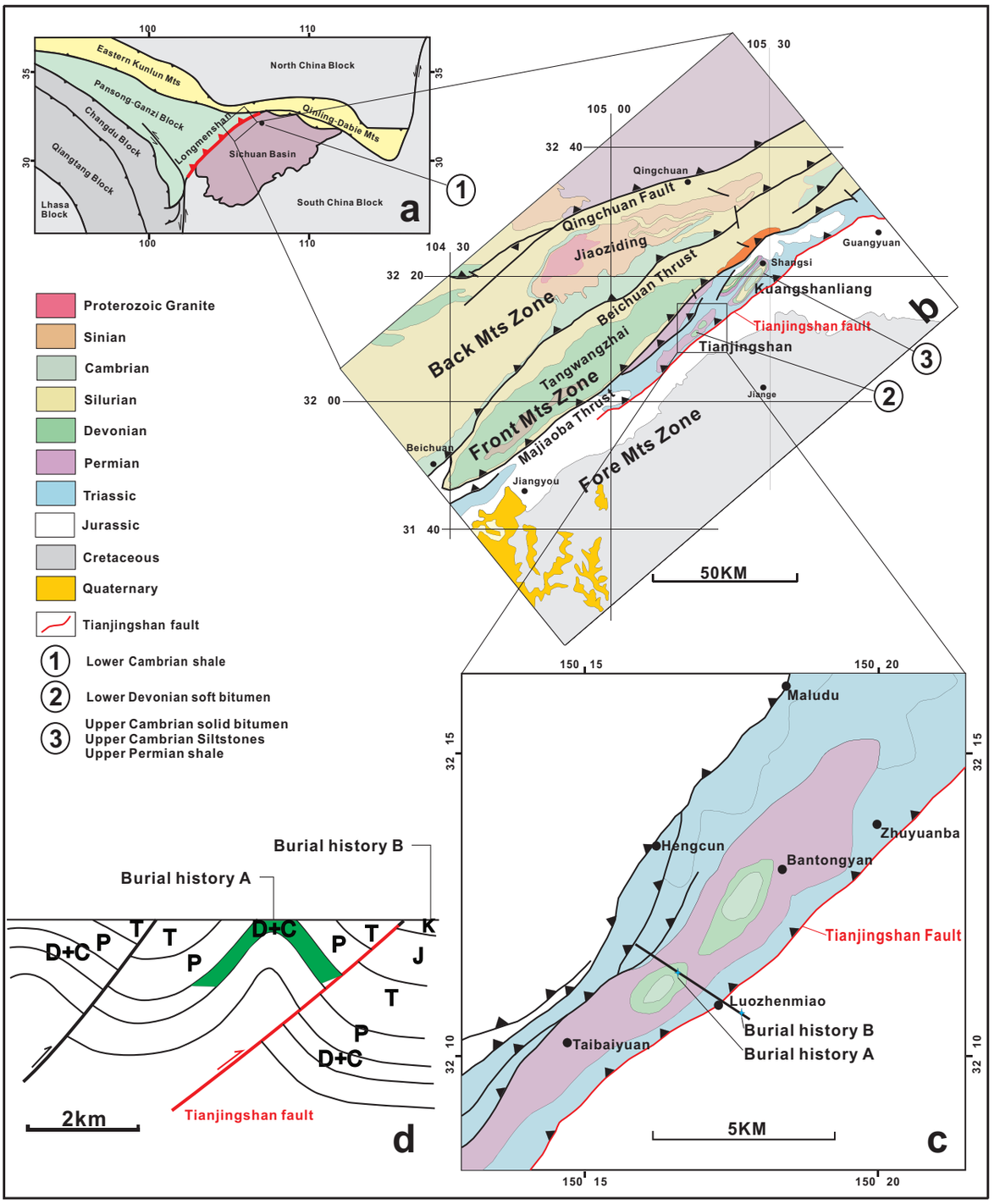

Fig.2. Location maps of the studied area: (a) regional map of the Sichuan Basin and the Longmenshan fold belt to the NW; (b) map showing structural elements in the northern part of the Longmenshan fold belt; (c) location map of the Tianjingshan fault and anticline showing the locations (A and B) at which the burial history was reconstructed (see text for details); (d) cross section of the Tianjingshan anticline; line of section in Fig 2c. (Modified from Jia *et al*., 2006, and Deng *et al*., 2008).

2008; Liu *et al*., 2010). However important problems have yet to be resolved such as the occurrence of low maturity soft bitumen in high maturity reservoir strata; whether both types of bitumen with different maturities were sourced from a single set of source rocks which are currently overmature; and the oil charge history of the reservoirs.

In this paper, we investigate the organic geochemical characteristics of the soft and solid bitumens which occur at Tianjingshan and nearby

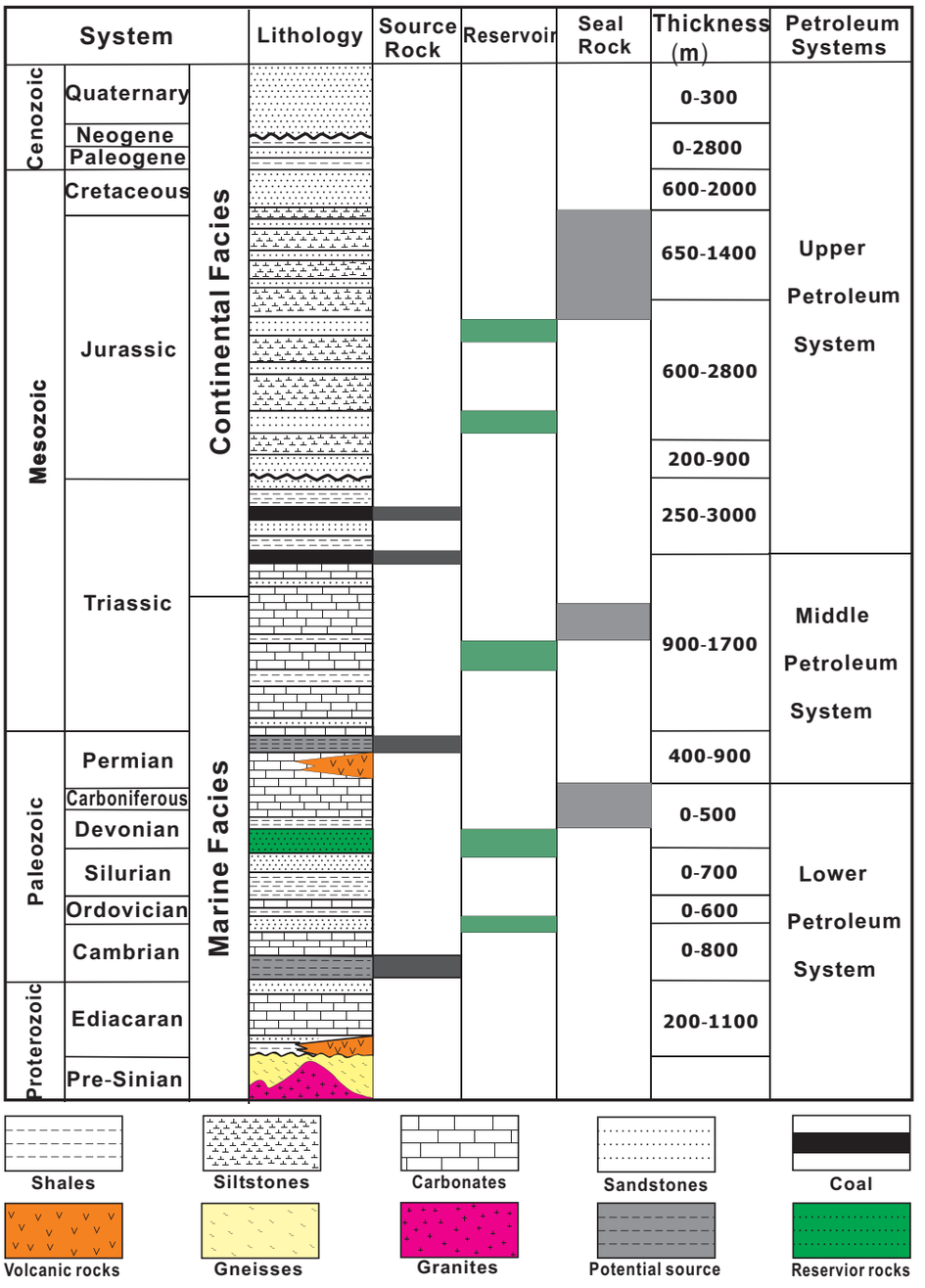

Fig.3. Schematic diagram showing the stratigraphy and petroleum systems of the western Sichuan Basin (modified from Jia *et al.*, 2006)

locations. Analyses of fluid inclusions in the Lower Devonian reservoir sandstones are presented. Burial and hydrocarbon generation histories of potential Palaeozoic source rocks were modelled and oil charging histories were assessed.

GEOLOGICAL SETTING

The SW-NE trending Longmenshan fold-thrust belt (Jia *et al.*, 2006; Huang *et al.*, 2009) at the NW margin of the Sichuan Basin is about 500 km long and up to 50 km wide (Fig. 2a), and is characterized by large-scale SW-NE trending folds and reverse fault systems (Fig. 2b). The structural evolution of this fold-thrust belt is still debated although a general model is now widely accepted (Tong *et al.*, 1997; Jia *et al.*, 2006; Huang *et al.*, 2009). Part of the Upper Cambrian and all of the Ordovician and Silurian successions are absent due to uplift and erosion during the Late Silurian Caledonian orogeny (Wang *et al.*, 2005; Pang *et al.*, 2010). Pre-Mesozoic (from Ediacaran to Permian) regional extension was accommodated by

major normal faults whose syndepositional activity controlled patterns of sedimentation (Li *et al*., 2012) and a Devonian – Permian succession is well developed in this region (Jia *et al*., 2006). Crustal shortening during the Indosinian orogeny (Late Triassic) resulted in the formation of the NE-SW trending Qingchuan, Beichuan and Majiaoba thrust belts (Li *et al*., 2012) (Fig. 2b). The controlling faults have been active to Recent times, resulting in uplift and erosion of the Mesozoic and Cenozoic intervals.

The Tianjingshan fault is a second-order fault in the Majiaoba thrust belt, and began to develop as a NE-SW oriented normal fault during the Permian Hercynian orogeny (Xiao *et al*., 2012). Permian to middle Triassic deposits thicken in the hanging wall of the fault. Thus the lower-middle Triassic interval is 3500-4000 m thick in the hanging wall but 1500-2000 m thick in the footwall (Xiao *et al*., 2012). During the Indosinian orogeny (Late Triassic), the fault was reactivated in a reverse sense and a hanging-wall anticline developed; Mesozoic and/or Palaeozoic strata were variably eroded (Sun *et al*., 2010; Xiao *et al*., 2012). However, Jurassic and Cretaceous deposition continued in the footwall (ECPGC, 1993). Subsequently, the Tianjingshan area was uplifted as a result of the Himalayan orogeny (Cenozoic), and the shallowest part of the stratigraphy was eroded resulting in the present-day structural configuration (Fig 2b).

Stratigraphy

Fig. 3 is a schematic diagram illustrating the stratigraphy and petroleum systems of the western Sichuan Basin. In the Longmenshan fold-thrust belt, organic-rich black shales in the Lower Cambrian Jiulaodong Formation, about 100 m thick, are considered to have source rock potential (Wang *et al*., 2005; Xie *et al*., 2003; Teng *et al*., 2008). The overlying Upper Cambrian Xixiangchi Formation (about 500 m thick) includes siltstones and fine-grained sandstones. Ordovician and Silurian strata are largely absent due to uplift and erosion during the Caledonian orogeny; the unconformably-overlying Lower Devonian Pingyipu Formation shallow-marine sandstones are about 150 m thick, and are overlain by Upper Devonian grey mudstones and siltstones (about 100 m thick). Carboniferous and Lower Permian strata consist of limestones and marlstones up to 50 m thick. These are overlain by lagoonal black shales and siliceous shales in the Upper Permian Dalong Formation (ca. 40 m thick) which are also considered to be potential source rocks (Xie *et al*., 2003; Wang *et al*., 2005; Teng *et al*., 2008).

The Lower-Middle Triassic stratigraphic succession includes neritic limestones interbedded with sandstones and shales with a total thickness of over 800 m. The Upper Triassic consists of marine and continental (transitional) sediments including the Xujiahe Formation dark-coloured mudstones and coals. The overlying Jurassic and Cretaceous fluvio-lacustrine sediments comprise sandstones, siltstones and mudstones. Jurassic strata have a thickness of up to 4000 m. The Lower Cretaceous is up to 2000 m thick; the Upper Cretaceous is mostly eroded; Cenozoic outcrops are confined to the SW of the basin and are not present in the studied area.

Petroleum geology

Little information is available concerning the petroleum systems in the Longmenshan belt (Chen *et al*., 2005; Jia *et al*., 2006). Organic-rich shales (Lower Cambrian and middle Permian) and Upper Triassic coaly intervals are beleived to be potential source rocks (Xie *et al*., 2003; Teng *et al*., 2008), and may supply hydrocarbons within separate petroleum systems (Fig. 3) (Liu *et al*., 2003; Qu *et al*., 2004; Huang and Wang; 2008; Rao *et al*., 2008; Liu *et al*., 2010; Zeng *et al*., 2010). Sandstones, siltstones and carbonates in the Upper Cambrian, Lower Devonian, Lower Triassic, Upper Jurassic and Cretaceous intervals are potential reservoir rocks (Xu *et al*., 2005; Sun *et al*., 2010). Seals are provided by middle Devonian marine mudstones and argillaceous limestones, middle Triassic gypsum and upper Jurassic to Cretaceous mudstones.

The bitumens which are present in the Upper Cambrian siltstones and Lower Devonian sandstones are believed to have been sourced from Lower Cambrian black shales (e.g. Liu *et al*., 2003; Huang and Wang; 2008; Rao *et al*., 2008; Liu *et al*., 2010). Solid bitumen is present in Upper Cambrian siltstones in the Kuangshanliang area (Fig.2) and also in Lower Devonian sandstones at Tianjingshan (Wang *et al*., 2005). Soft lower maturity bitumen occurs in Lower Devonian sandstones at Tianjingshan (Liu *et al*., 2003; Wang *et al*., 2003; Deng *et al*., 2008; Huang *et al*., 2008; Liu *et al*., 2010).

MATERIALS AND METHODS

Samples

For this study, black shales from the Lower Cambrian Jiulaodong Formation and the Upper Permian Dalong Formation were analysed using standard organic geochemical techniques to assess their source rock potential. Owing to the absence of suitable outcrops in the Longmenshan fold-thrust belt, the Lower Cambrian black shale samples were collected from a road cutting near Nanjiang, about 100 km from Tianjingshan (location in Fig. 2a), where about 50 m of Lower Cambrian black shales are exposed. Four black shale samples were collected from this section (Fig. 4a). Seven black shale samples from the Upper

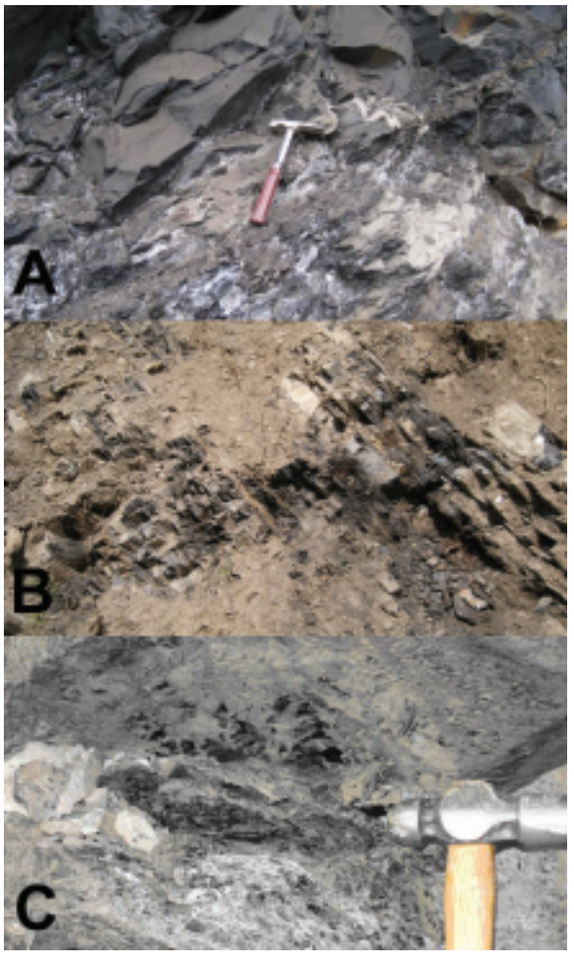

Fig. 4. Outcrop photographs of: (A) Lower Cambrian black shales at Nanjiang; (B) Upper Permian black shales near Shangsi village in the Kuangshanliang area; and (C) Lower Devonian bitumen-bearing sandstones in the Tianjingshan anticline. For locations, see Figs 2a and 2b.

Permian Dalong Formation were collected from a location near Shangsi village in the Kuangshanliang area (location in Fig. 2b) where about 15 m of unweathered shales are exposed in a road cutting (Fig. 4b).

Samples of both high- and low-maturity bitumen were also analysed. The high maturity bitumen sample was taken from a bitumen vein in Upper Cambrian Xixiangchi Formation siltstones in a shallow pit near Shangsi village, about 20 km from the Tianjingshan anticline. Samples of low maturity bitumen were recovered from Lower Devonian Pingyipu Formation sandstones at an open-cast mine at the Tianjingshan anticline (Fig. 4c; location in Fig. 2b).

Fluid inclusions in the Lower Devonian Pingyipu Formation sandstone samples from the Tianjingshan anticline were studied by microthermometry. Burial and thermal histories at two key locations were also reconstructed (see below).

Methods

An IFP Rock-Eval VII instrument was used to assess the hydrocarbon generation potential of Lower Cambrian and Upper Permian black shales. Standard IFP55000 was applied to calibrate the instrument before and after sample analyses.

Bitumen reflectance was measured on polished blocks with a *Leitz* microphotometric system. The equipment was calibrated by a *Leitz* saphire standard with R_o = 0.522%. The photometer used can read a spot with a diameter of 5μm at 546 nm on the sample surface using an objective of 125 × 0.85 in oil immersion (ne = 1.518).

Lower Devonian sandstones and fluid inclusions were examined on double-polished thin sections using a *Leica DMRX MPV III* microspectrometer equipped with a high pressure mercury vapour lamp and a *Leica H3* filter cube (No. 513827), which includes an excitation filter of 420-490 nm, a dichromatic filter of 510 nm and a suppression filter of 515 nm. Homogenisation temperatures of the inclusions were obtained using a *Linkam THMSG 600* heating stage attached to a *Leica DMRX* microscope. A *Linkam TMS 94* control unit was used. During the measurements, a heating rate of 5 - 10°C/min used at the beginning was decreased with rising temperature to 1°C / min near homogenisation, and the temperature was held constant for about 30 s after it was achieved.

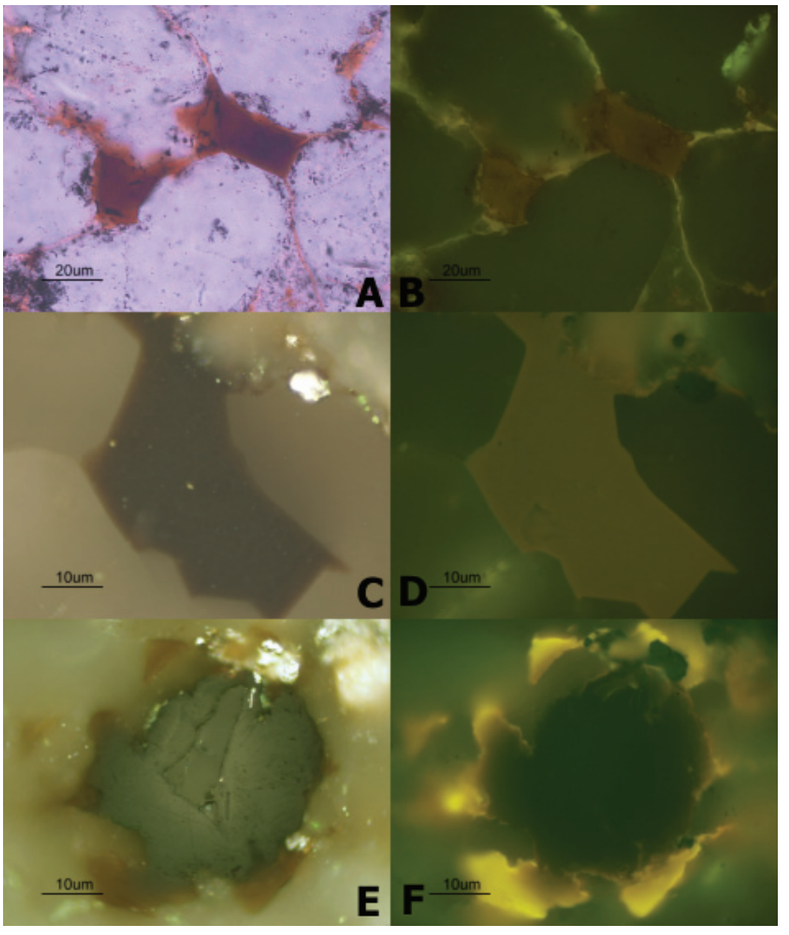

Fig. 5. Photomicrographs of different types of bitumen from Lower Devonian sandstones and Upper Cambrian siltstones analysed. A. Soft low-maturity bitumen from Lower Devonian sandstones, transmitted light; B. Same field as A, fluorescence illumination; C. Low R_o bitumen from Upper Cambrian siltstones, reflected light; D. Same field as C, fluorescence illumination; E. Higher R_o bitumen from Upper Cambrian siltstones, reflected light; F. Same field as E, fluorescence illumination.

Raman spectra from the fluid inclusions were obtained using an *ARAMIS* Raman microprobe from Horiba Jobin Yvon, equipped with an Olympus photometer. An LMPlanFL N objective (50×/0.5) and a laser source with a wavelength of 532 nm linked to the microprobe were used. A silicon slice working standard was used to calibrate the synapse CCD detector. The measurements were made under the following conditions: 40 s exposure, accumulation of 2×7, binning 1, hole 200, slit 100, grating 1800, filter D 0.6.

A *ThermoQuest Flash EA1112 Series* C N elemental analyzer linked to a *Finnigan Delta Plus XL* Isotope Ratio Mass Spectrometer (IRMS) via a *Finnigan MAT ConFlo III* unit was used for the measurement of carbon isotope ratios in the kerogen of the Upper Permian Dalong Formation shale and of the bitumens. The CO_2 gas converted from the samples after combustion under a flow of helium and oxygen in an oxidation tube at 900°C was measured. To ensure accuracy of measurement, the EA-IRMS system was calibrated by a working standard before measurements of the samples. The CO_2 reference was also calibrated against the NBS 22 oil standard.

Burial histories were reconstructed using PetroMod 1D software. The input data for the modelling included depositional and eroded thicknesses during different geological time-periods, as well as the lithologies of the relevant strata. Two locations were selected for burial history modelling. The first was the core of the Tianjingshan anticline in the hanging wall of the Tianjingshan fault (location A, Figs 2c, d); the stratigraphic succession here was based on Jia *et al*. (2006). The other location was in the footwall of the Tianjingshan fault (location B, Figs. 2c,d); the stratigraphic framework for this location was provided by CNPC Southwestern Company (*unpublished data*).

The thermal maturation history was modelled using the EasyR_o approach (Sweeney and Burnham, 1990). The modelling combined the burial history with the palaeo geothermal gradient. Since there is lack of palaeo geothermal data in the studied area, a

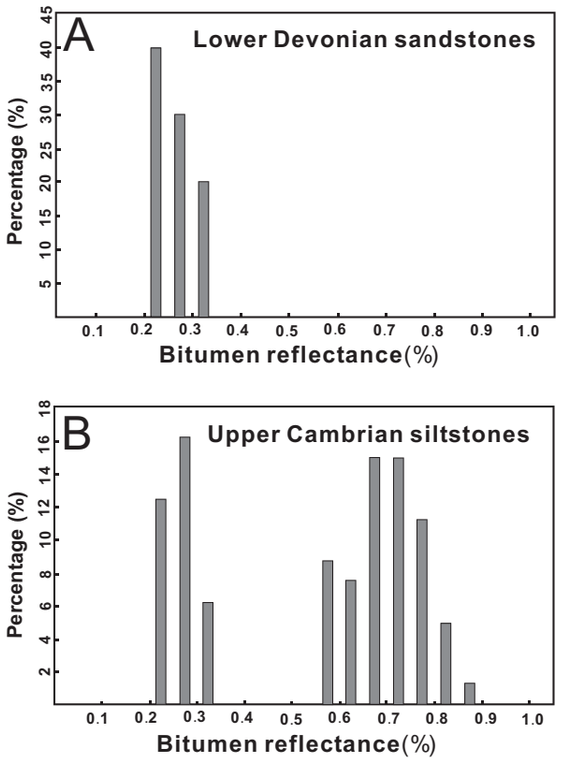

Fig. 6. Histograms of reflectance (BR_o) of: (A) low-maturity "soft" bitumen from Lower Devonian sandstones (average: 0.26% when converted to oil immersion reflectance); and (B) low- and high-maturity bitumen from Upper Cambrian siltstones (average reflectance under oil immersion: 0.27% and 0.66%, respectively).

simplified model was applied: 3.0 °C /100 m before 96 Ma; 2.8 °C / 100 m from 96 to 65 Ma; 2.2 °C / 100 m from 65 Ma to the present day; and 15°C for the palaeo surface temperature, as proposed by Wang and Xiao (2010) for the Sichuan Basin.

RESULTS

Bitumen characteristics

Low-maturity bitumen in the Lower Devonian sandstones was soft and had low BR_o (bitumen reflectance) values. The bitumen was russet-coloured in transmitted light and brownish-yellow in fluorescent light (Fig. 5a, 5b). Because it was soluble in the immersion oil, the reflectance was measured in air. The results range from 3.2-4.4% (average: 3.7%), equivalent to 0.22-0.31% (average 0.26%) when converted to oil immersion reflectance (Fig. 6A). The bitumen is very soft and can be completely dissolved in dichloromethane, and is more correctly described as an asphaltic heavy oil. It is referred to here as "soft bitumen" to distinguish it from the higher maturity solid bitumen which occurs in Upper Cambrian siltstones (see below).

Liu *et al*. (2003) reported the presence of solid high-maturity bitumen (about 1.0% BR_o) in Lower Devonian sandstones in the study area; however this was not encountered in the present study.

Solid bitumen in the Upper Cambrian siltstones was black in transmitted light, dark grey in reflected light and had little fluorescence (Fig. 5e, 5f). Reflectance under oil immersion ranged from 0.54 to 0.85% (average: of 0.66%) (Fig. 6b). Lower maturity soft bitumen similar to that in Lower Devonian sandstones was also present (Fig. 5c, 5d) and had reflectance of about 0.22-0.32% (average 0.27%) converted into oil immersion reflectance from measured air reflectance (Fig. 6b).

Source rocks

(i) Lower Cambrian black shales

Lower Cambrian black shales samples from Nanjiang have a TOC of 3.41- 4.53% (average: 3.8%). Both Rock-Eval S_1 (residual hydrocarbon) and S_2 (pyrolysis hydrocarbon) were zero (Table 1). Pyrobitumen was the major maceral (Fig. 7A and 7B), with some dispersed micrinite derived from alginite or amorphinite. The measured reflectance value of the pyrobitumen varies from 3.53 to 4.03% (Table 1), giving an equivalent vitrinite reflectance of 2.71 -3.04 %. The Lower Cambrian black shales can be interpreted as overmature source rocks containing Type I/II_1 kerogen.

(ii) Upper Permian black shales

The samples of the Upper Permian Dalong Formation shales analysed contain TOC of 2.08% to 9.79% (average: 4.67%). HI ranges from 91 to 245 mg/g, with an average of 175 mg/g, and vitrinite reflectance ranges from 0.64-0.87% (Table 1). The shales contain Type III kerogen with vitrinite as the main component (Fig. 7C) and some exinite (Fig. 7D). These observations are consistent with Xie (2003) who reported that the Dalong Formation contains Type II_2 - III kerogen.

Reservoir rocks

Petrological observations show that the Lower Devonian sandstones contain major quartz and minor orthoclase and can be classified as quartz arenites. Minerals in the sandstones are medium to fine-grained (grain diameters from 50 to 500 μm). Quartz clasts are in general rounded with siliceous cement. Bitumen is present in proportions of about 2-5% (Fig. 8a, 8b).

The Upper Cambrian siltstones were dominated by quartz with less common carbonate minerals, feldspars and muscovites. Grain diameters range from 5 to 30 μm. The grains are poorly rounded and have argillaceous cements. Minor quantities of bitumen (less than 1%) were observed (Fig. 8c, 8d).

Sample No	location	Age	S1 (mg/g)	S2 (mg/g)	S3 (mg/g)	Tmax oC	HI (mg/g)	OI (mg/g)	TOC (%)	VRo/BRo (%)*
SS-1	Shangsi	U. Permian	0.61	6.39	0.29	435	181	12	4.06	0.72
SS-2			0.13	2.47	0.83	437	91	41	3.33	0.79
SS-3			0.15	12.34	0.44	437	149	31	9.79	0.87
SS-4			0.12	5.13	1.11	437	220	25	2.94	0.64
SS-5			0.13	2.73	2.54	439	146	30	2.08	0.72
SS-6			0.14	4.86	0.58	442	189	11	3.34	0.84
SS-7			0.31	15.3	0.56	439	245	13	7.13	0.65
NJ-1	Nanjiang	Lr Cambrian	0.01	0	0.39	/	0	9	4.53	3.53
NJ-2			0	0	0.24	/	0	6	3.98	3.69
NJ-3			0	0	0.16	/	0	5	3.41	4.03
NJ-4			0	0	0.21	/	0	6	3.29	3.79

* VRo for Upper Permian shale, BRo for Lower Cambrian shale.

Table 1. TOC, maturity and Rock-Eval data for the Upper Permian and Lower Cambrian black shales from the study area.

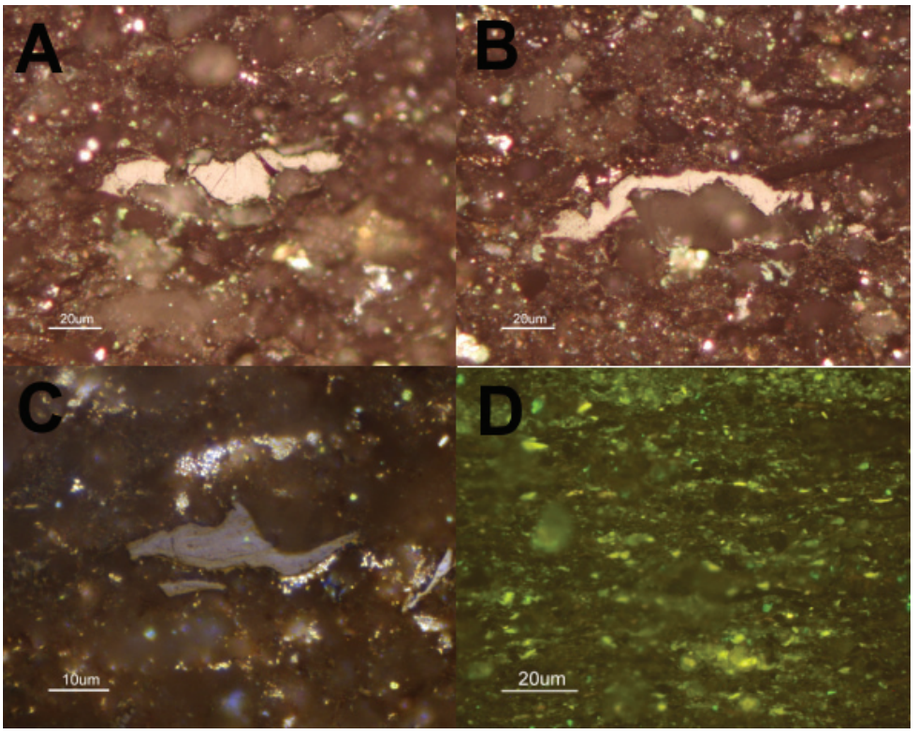

Fig.7. Photomicrographs of macerals in Lower Cambrian black shale and Upper Permian black shale.
A and B: pyrobitumen, reflected light, Lower Cambrian black shale, Nanjiang village;
C. vitrinite, reflected light, Upper Permian black shale, Shangsi village;
D. exinite, fluorescence light, Upper Permian black shale, Shangsi village.

Two types of hydrocarbon inclusion were identified in micro-fractures in quartz grains in the Lower Devonian sandstones from Tianjingshan: liquid and gaseous (Fig. 9). The liquid hydrocarbon inclusions had a yellow fluorescence (Fig. 9A, 9B) characteristic of crude oil (McLimans *et al*., 1987; Stasiuk and Snowdon *et al*., 1997; George *et al*., 2001; Blanchet *et al*., 2003). The inclusions had a wide range of homogenisation temperatures from 88 to 155 °C with a main range from 120 to 145 °C (Fig. 10). This suggests that the inclusions were trapped from fluids with a range of temperatures over a long period of time, or that "necking" occurred during cooling.

Rare aqueous inclusions were also identified in the Lower Devonian sandstones, and some coexist with petroleum inclusions. Homogenisation temperatures of the aqueous inclusions are in the range 125-155 °C (Fig. 10), similar to the homogenisation temperatures of the liquid petroleum inclusions.

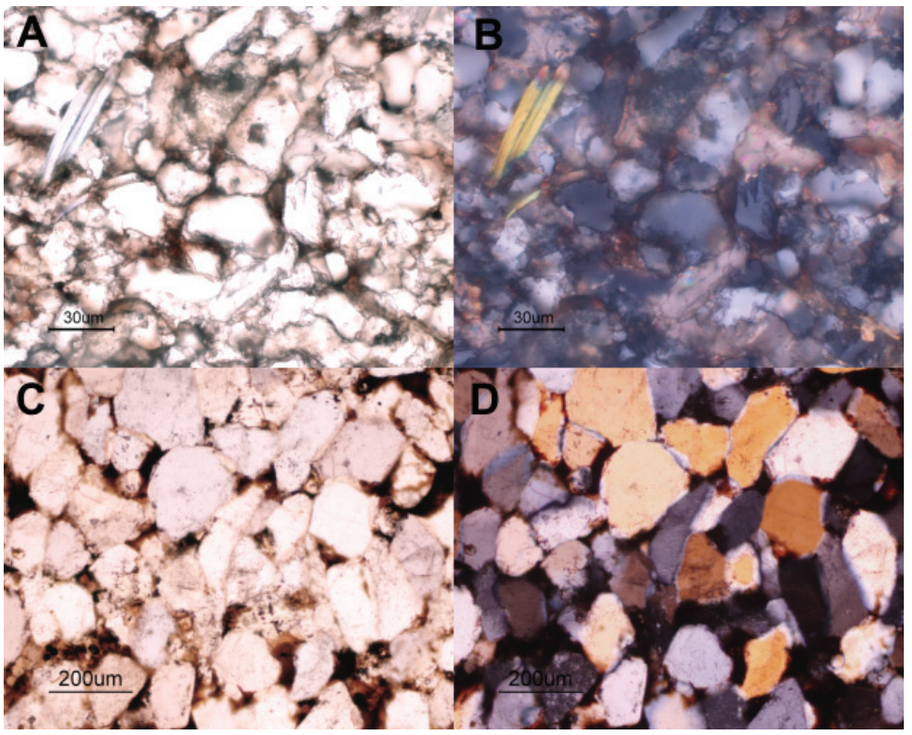

Fig.8. Photomicrographs of Lower Devonian sandstone and Upper Cambrian siltstone reservoir rocks showing petrological characteristics. A. Upper Cambrian siltstone, plane polarized light; B. Same field as A, XPL; C. Lower Devonian sandstone, PPL; D. Same field as C, XPL.

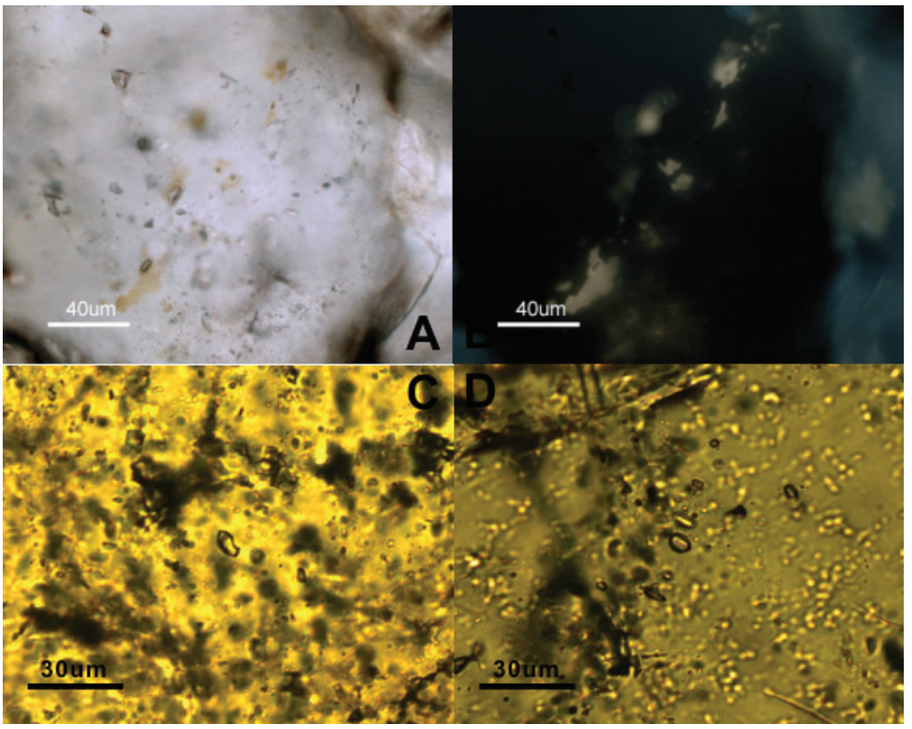

Fig. 9. Photomicrographs of hydrocarbon inclusions from the Lower Devonian sandstones. A. Liquid petroleum inclusions, transmitted light; B. Same field as A, fluorescence illumination; C and D. Gaseous hydrocarbon inclusions, transmitted light.

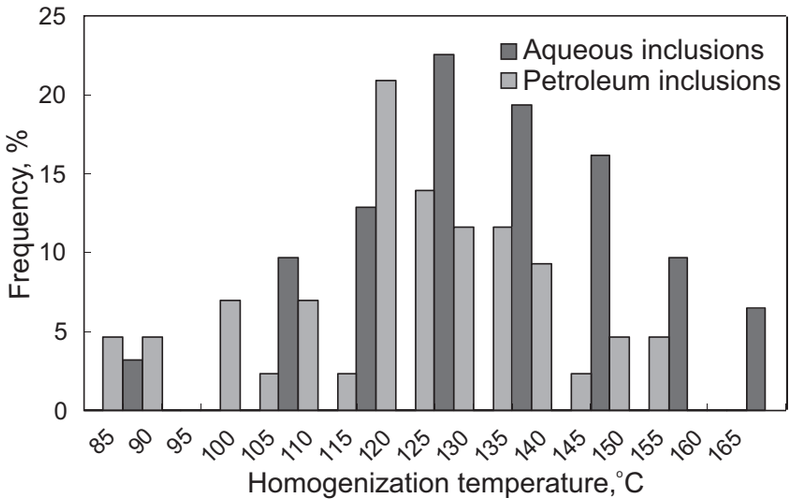

Fig.10. Histogram of homogenisation temperatures of petroleum inclusions and coexisting aqueous inclusions from the Lower Devonian sandstones, showing main temperature ranges of 120 -145 °C and 125-155 °C for petroleum inclusions and aqueous inclusions, respectively.

Gaseous hydrocarbon inclusions present are transparent and dark-edged (Fig. 9C, D). They are usually ellipsoidal or negative-crystal shaped, but some are irregular. Laser Raman spectrometry was used to identify components in typical inclusions. The results show that methane is the dominant component, with minor carbon dioxide, aromatic hydrocarbons and asphaltene. The Raman shift of methane in a gaseous hydrocarbon inclusion is 1910-1918 cm^{-1}, and decreases with increasing internal pressure (Fabre *et al*., 1992; Brunsgaard *et al*., 2001, 2002; Liu *et al*., 2010). The Raman shift of the methane in the gaseous hydrocarbon inclusions is 2911.1 cm^{-1} (Fig. 11), indicating relatively high pressure conditions during (or subsequent to) the time when the inclusions were trapped.

These characteristics of the gaseous hydrocarbon inclusions are similar to those of high density methane inclusions formed by thermal cracking of petroleum inclusions in the *Puguang* gasfield, NE Sichuan Basin (Liu *et al*., 2010). The coexistence of hydrocarbon gas and asphaltene indicates that it is quite possible that the gaseous hydrocarbon inclusions occurring in the Lower Devonian sandstones were derived from a petroleum inclusion which experienced high temperature conditions (>170-180 °C) after it was trapped, and trapping should be much earlier than that of the associated liquid petroleum inclusions.

Carbon isotope ratios

Stable isotope ratios were measured on bitumen samples from the Lower Devonian and Upper Cambrian reservoir rocks, and on kerogen from the Upper Permian black shales. Averages bulk carbon isotope ratios of the two types of bitumen are -35.56 to -35.58 ‰ and -35.71 to -35.73 ‰, respectively. The kerogen in the Upper Permian shales has an average isotope ratio value of -27.1 to -27.7 ‰.

Stable isotope ratios for kerogen in the Lower Cambrian black shales from the studied area were not examined in the present investigation. However previous studies have shown that the average bulk isotopic values of kerogen from these shales is -31.2 ‰ to -34.4 ‰ (Li *et al*., 1999; Teng *et al*., 2008).

Thermal and maturation history modelling

Fig. 12 illustrates the burial histories of the modelled locations in the hanging wall (A) and footwall (B) of the Tianjingshan fault (locations in Fig. 2c). In the hanging wall location, maximum burial (5900 m for the Lower Cambrian, 3700 m for the Upper Permian) occurred at the end of the middle Triassic. Subsequent uplift resulted in the erosional removal of a section about 4800 m thick comprising the upper Devonian to middle Triassic. In the footwall location by contrast, progressive burial took place throughout the Mesozoic and the Mesozoic reaches a thickness of over 6000 m. Minor uplift during the Cenozoic resulted in the erosion of about 300-400 m of section.

The thermal maturation histories of the Lower Devonian sandstones in the hanging wall, and that of the Lower Cambrian black shales in the hanging wall and footwall, are presented in Figs 13 and 14, respectively. In the hanging wall, modelling shows that the Lower Devonian sandstones reached an EasyR_o value of 1.63 % at the end of the Late Triassic (about 199 Ma) (Fig. 13b). The Lower Cambrian black shales in the hanging wall reached the main stage of oil generation in the Early-mid Triassic (243-226 Ma) with EasyR_o values ranging from about 0.70% to 1.23%. The EasyR_o value reached 1.50% at about the beginning of the Late Triassic (~220 Ma), and

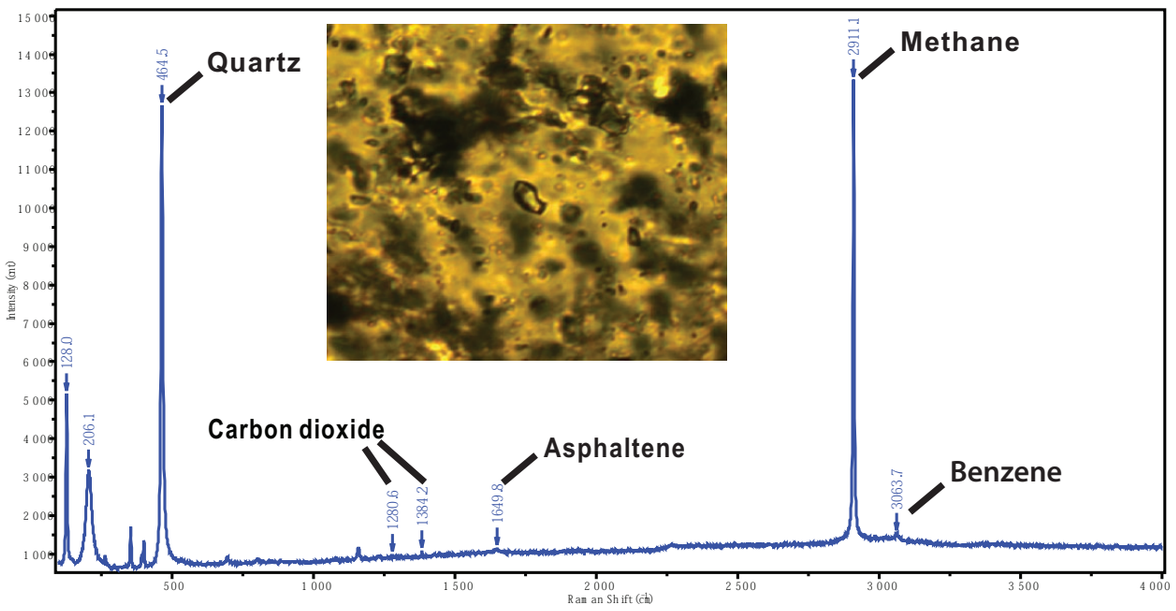

Fig. 11. Raman spectrum of a gaseous hydrocarbon inclusion showing that methane is dominant, with minor carbon dioxide, aromatic hydrocarbons and asphaltenes.

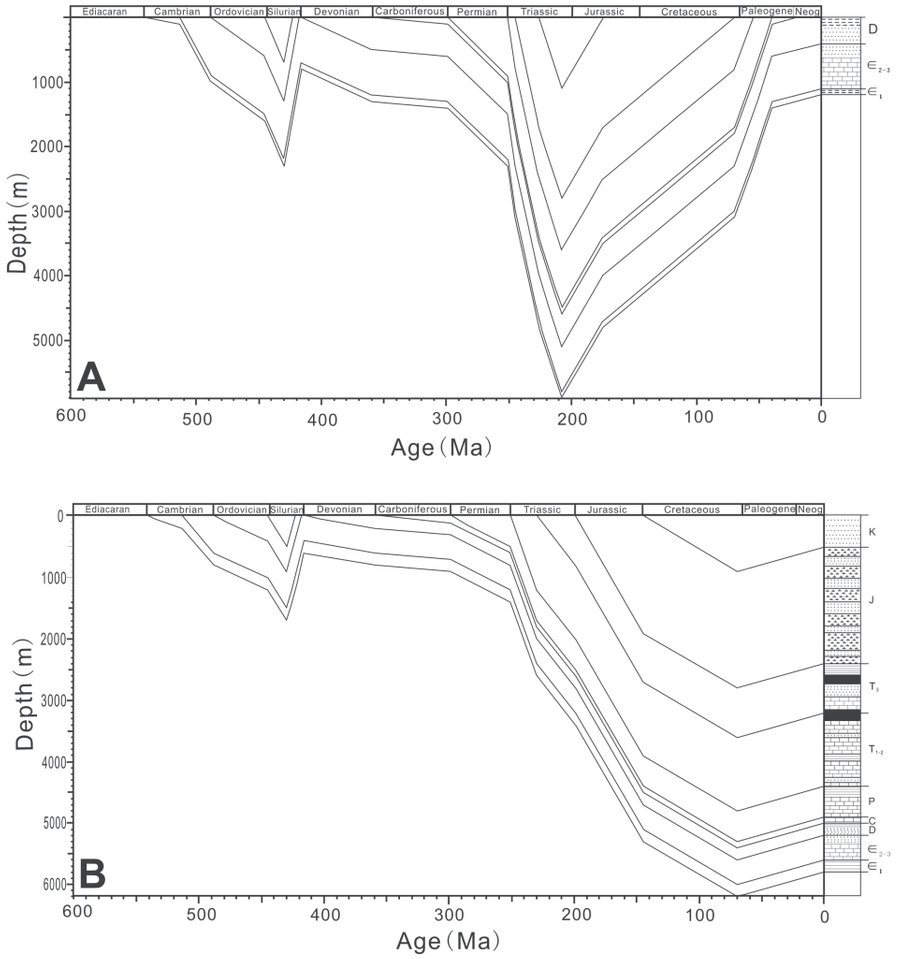

Fig. 12. Modelled burial histories of locations in the hanging wall (A) and footwall (B) of the Tianjingshan fault. Locations marked in Fig. 2c.

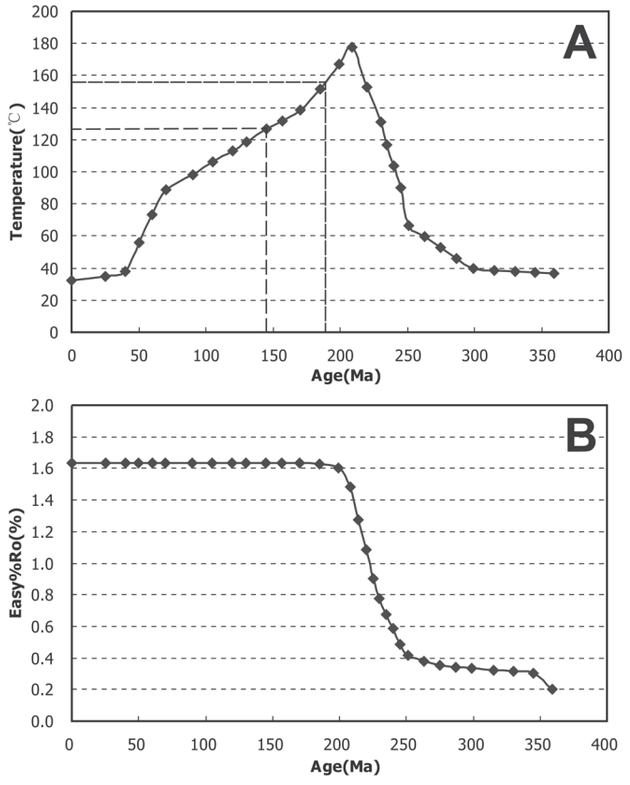

Fig.13. Thermal history (A) and EasyR_o maturation history (B) of the Lower Devonian reservoir rocks in the Tianjingshan anticline. The homogenisation temperature of petroleum inclusions is 125~155°C, corresponding to a charge time of about 190-145 Ma.

over 2.0% by the end of the Late Triassic, reaching the dry gas stage (Fig. 14).

The Lower Cambrian shales in the footwall however are modelled to have had a different maturation history, and only just began to generate oil in the Late Triassic when uplift began (~208-199 Ma), reaching the main stages of oil generation in the Early-mid Jurassic (~199-160 Ma), with EasyR_o values ranging from 0.73% to 1.19 %. The shales became overmature by the end of the Jurassic. Present-day EasyR_o is over 2.6% (Fig. 14).

DISCUSSION

Source of the bitumen

Previous studies (Liu *et al*., 2003; Huang and Wang, 2008; Rao *et al*., 2008; Liu *et al*., 2010) have investigated the molecular geochemical characteristics of the Lower Devonian soft bitumen at Tianjingshan and the Upper Cambrian solid bitumen at Kuangshanliang. Similarities in their gonane and terpane biomarker characteristics and in their pyrolysis gas chromatograms suggests that both bitumens may have originated from Lower Cambrian source rock (Liu *et al*., 2003). Both bitumens are C_{29}-gonane dominant with a high content of C_{35} homohopane. This is sharp contrasts with biomarkers in the Upper Permian black shale which shows a "V" profile in the C_{27}-C_{28}-C_{29} gonane distribution and no dominance of C_{35} homohopane (Rao *et al*., 2008; Liu *et al*., 2010). Huang and Wang (2008) showed that alkanes in the Lower Devonian bitumen are characterized by short chain lengths with a peak at nC_{17}, and are dominated by phytane. This indicates that the Lower Devonian bitumen has an algal affinity, possibly originating from a Lower Palaeozoic source.

The carbon isotope data in the present study indicates that both types of bitumen were derived from a Lower Cambrian shale source. In general, the carbon isotope value of a crude oil is 1-2 ‰ lighter (i.e. $\delta^{13}C$ is more negative) than the value of its source kerogen, while the value of solid bitumen is 2-3 ‰ heavier than the value of the crude oil from which it is derived (Machel *et al*., 1995; Cai *et al*., 2006). The isotope ratio value of the solid bitumen should therefore be 1-2 ‰ heavier than the value of its source kerogen. The bulk carbon isotope ratios of the crude oil and bitumen generated from the Upper Permian source rocks should therefore not be lighter than -30 ‰. However, this is not consistent with the isotope ratio values of either type of bitumen. The bulk isotope value of heavy oil or bitumen from the Lower Cambrian source rocks should however be in the range -31 ‰ to -36 ‰, which is quite close to the

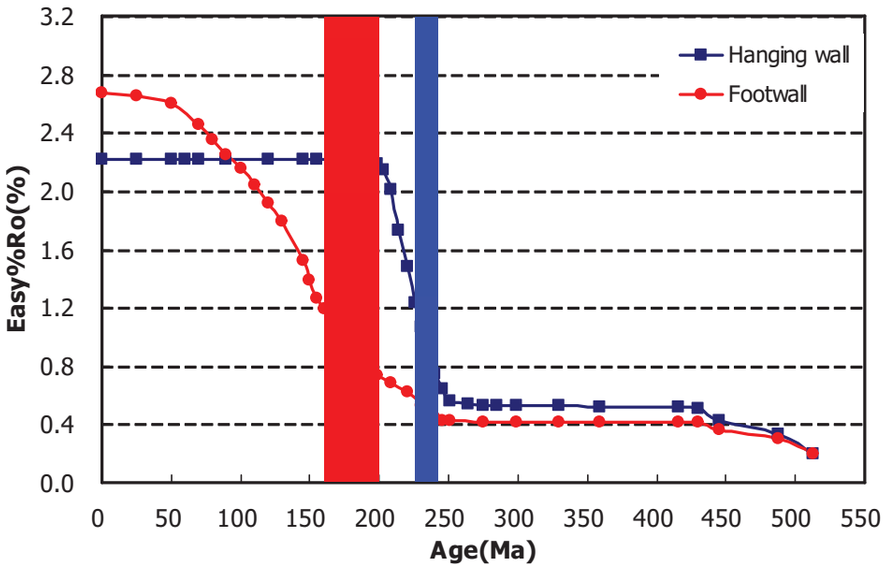

Fig. 14. Easy R_o evolution histories of Lower Cambrian black shales in the hanging wall and footwall of the Tianjingshan fault. The blue and red bars show the main hydrocarbon generation stages of Lower Cambrian shales in hanging wall and footwall locations, respectively.

recorded isotope values of the bitumens. The isotope ratios therefore indicate that the two types of bitumen were generated by the Lower Cambrian shales and not the Upper Permian shales.

Oil charge history

Multicharge history in a single petroleum reservoir has been demonstrated by the occurrence of two sets of inclusion oils and other geological evidence in the North Atlantic (e.g. the Jeanne d'Arc Basin, Newfoundland; the Porcupine Basin, Ireland; the *Clair* field, West of Shetland; and the Kangerlussuaq Basin, East Greenland: Parnell *et al*., 1998; Parnell *et al*., 2001; Feely *et al*., 2003; Jonk *et al*., 2005; Baron *et al*., 2008; Blamey *et al*., 2009). In the present study, the presence of bitumens with widely different maturities, and of two types of fluid inclusions in the Lower Devonian sandstones, indicates that there were two phases of oil charging at the Tianjingshan anticline. The solid higher maturity bitumen and the gaseous inclusions are interpreted to be derived from an early oil charge. The soft low maturity bitumen and the liquid petroleum inclusions were preserved because they did not experience high temperature conditions and are interpreted to result from a later oil charge.

The relative timing of the oil charge events can be deduced by combining observations about the fluid inclusions with the thermal history of the reservoir rocks (Bodnar *et al*., 1990; Aplin *et al*., 2000; Parnell *et al*., 2001; Liu *et al*., 2003; Xiao *et al*., 2002, 2005; Mi *et al*., 2004; Tian *et al*., 2008). Preservation of the petroleum inclusions in the studied reservoir indicates they were not subsequently exposed to high temperature conditions. Thus, using the homogenization temperatures of the aqueous and liquid petroleum inclusions, the trapping time of these inclusions is determined to be approximately 190 to 145 Ma, i.e. in the Early-mid Jurassic (Fig. 13 and Fig. 15C).

A trapping time for gaseous inclusions is more difficult to determine because no accompanying aqueous inclusions were found. As discussed above, the gaseous inclusions were formed by high-temperature cracking of liquid petroleum in inclusions, or by the trapping of cracked gas in the pore spaces. Until the Late Triassic, Lower Devonian reservoir sandstones in the hanging wall of the Tianjingshan fault were buried progressively and experienced increasing temperatures up to about 180 °C with an EasyR_o of > 1.6% (Fig. 13). This temperature was above the threshold of oil cracking into gas (Barker, 1990; Hayes, 1991; Pepper *et al*., 1995; Schenk *et al*., 1997). Therefore this oil charge event should have occurred before the Late Triassic when the reservoir was uplifted; it is inferred to have taken place in the Early to mid Triassic.

Thus the main stage of oil generation by the Lower Cambrian source rocks in kitchens in the hanging wall and footwall of the Tianjingshan fault were Early-mid Triassic and Early-mid Jurassic, respectively (Fig. 14). These coincide with the occurrence of the two oil-charge events in the Lower Devonian reservoir rocks in the Tianjingshan anticline. An early oil charge in the Lower Devonian sandstones originated from Lower Cambrian source rocks in hanging-wall kitchens. This early oil was thermally degraded in the reservoir to high-BR_o solid bitumen. The later oil charge, derived from Lower Cambrian source rocks

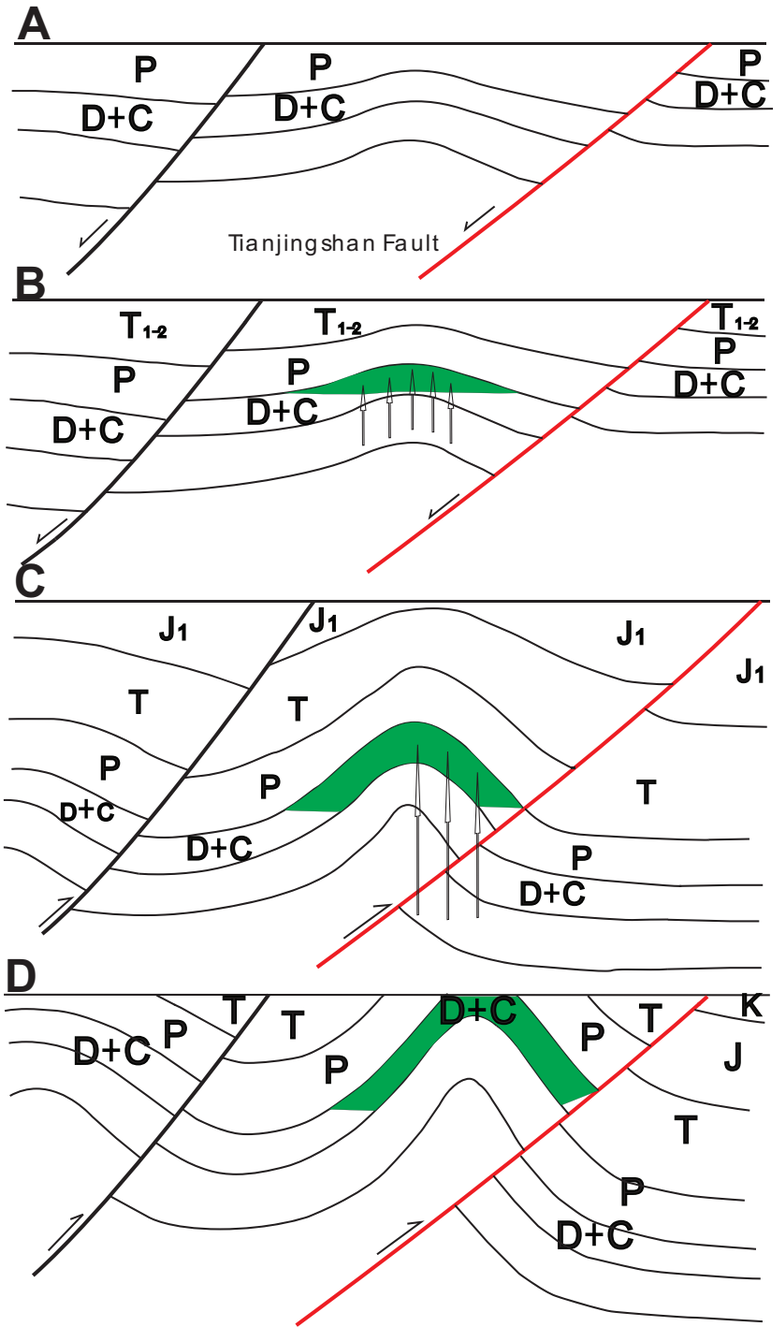

Fig. 15. Cartoon showing the formation and evolution of the Tianjingshan palaeo-oil accumulation. A. Formation of the Tianjingshan uplift; B. early oil charge in the Early-mid Triassic; C. Later oil charge in the Early-mid Jurassic; D. Formation of the present-day palaeo oil accumulation. See text for details.

in footwall kitchens, produced the less mature soft bitumen.

Bitumen formation and evolution

The formation and accumulation of bitumen in the Lower Devonian sandstones can therefore be understood in terms of a four-stage process (Fig. 15).

Stage 1: Formation of the Tianjingshan uplift. In the Early Palaeozoic, regional extension in the Tianjingshan area was accommodated by a series of normal faults. A stratigraphically-complete Lower Palaeozoic succession was deposited, but the Caledonian orogeny in the Late Silurian resulted in uplift of the area, and Silurian, Ordovician and part of the Upper Cambrian were eroded. Subsequently, the previously-formed normal faults were active during deposition of Devonian, Carboniferous and Permian strata (Fig. 15a)

Stage 2: Early oil charge and oil cracking. In the Early-mid Triassic, Lower Cambrian source rocks in

the hanging wall of the Tianjingshan Fault became progressively buried due to syndepositional fault activity and experienced increasing temperatures. Oil was generated, expelled, migrated and accumulated in Upper Cambrian – Lower Devonian reservoir rocks. Subsequent exposure to relatively high temperatures cracked this oil into gas and solid bitumen (Fig. 15B).

Stage 3: Later oil charge. The Tianjingshan fault was reactivated in a reverse sense at the end of the Late Triassic (Fig. 15C). The Lower Cambrian source rocks in footwall locations began to generate oil at the end of the Late Triassic, and reached the main oil generation stage in the Early-mid Jurassic. The generated oil migrated along the fault to Lower Devonian reservoir rocks in the hanging wall (Fig. 15C). The oil in this reservoir did not undergo thermal alteration and was preserved, because of continuous uplift of the hanging wall due to reverse fault activity.

Stage 4: Reservoir exhumation. During the Yanshan and Himalayan orogenies (Cretaceous and Cenozoic), the Tianjingshan area underwent compression and folding, and the region became uplifted and eroded. The Lower Devonian reservoir rocks were eventually exhumed (Fig. 15D) and the oil was biodegraded to soft low maturity bitumen.

Exploration significance

Precambrian and lower Palaeozoic black shales are present in the Sichuan and Tarim Basins (China), and in other areas including the South Oman Salt Basin, the NE Siberian Platform, the Gaspé Peninsula and Northern Poland (Zhang *et al*., 2000; Cai *et al*., 2008; Grosjean *et al*. 2009, 2012; Cai *et al*., 2009a,b; Xiao *et al*., 2005; Parfenova *et al*., 2010; Grundman *et al*., 2012). Some of these shales form excellent source rocks with high TOCs (Liu *et al*., 2003; Wang *et al*., 2007; Grundman *et al*., 2012). However, few commercial oil accumulations sourced by Lower Cambrian source rocks have so far been found. This is either because the source rocks are highly (or over) -mature, or because the oil generated has been destroyed during later tectonic or thermal events (Liu *et al*., 2003; Xiao *et al*., 2005; Huang *et al*., 2012; Grundman *et al*., 2012).

In the Tianjingshan area, however, soft bitumen and heavy oil derived from the Lower Cambrian source rocks has been preserved in an exhumed reservoir. Similar palaeo accumulations have been found in the Kuangshangliang and Houba areas of the Longmenshan foldbelt (Chen *et al*., 2005; Xu *et al*., 2005; Dai *et al*., 2007; Huang *et al*., 2008). About 260 oil and gas seepages and bitumen veins have been discovered between Guangyuan and Anxian (Wang *et al*., 2005) (locations in Fig. 2), some of which are thought to have been generated from Lower Cambrian source rocks. The model for the formation of the Tianjingshan palaeo accumulation presented here may be applicable to other areas in the Longmenshan foldbelt. Other palaeo accumulations sourced from Lower Cambrian source rocks may be found in preserved hanging wall anticlines.

Recent exploration of the Triassic Feixianguan Formation in the NE Sichuan Basin has resulted in the discovery of seven commercial gasfields (*Puguang, Wolonghe, Wubaiti, Shapingchang, Luojiazhai, Dukouhe* and *Tieshanpo*) with total resources of over 500×10^9 m^3 (Ma *et al*., 2005; Liu *et al*., 2008). Large quantities of solid bitumen are also present in this formation, indicating the former presence of a large-scale oil accumulation (Ma *et al*., 2005; Cai *et al*., 2005, 2006; Hao *et al*., 2008). However, the origin of the bitumen and the relationship between the bitumen and natural gas are not understood because little geochemical information has been obtained due to the high maturity of the bitumen (Cai *et al*., 2006; Hu *et al*., 2010). The approach used in this paper, based on pyrolysis analyses and kinetic modelling combined with thermal history reconstruction, may allow a better understanding of the origin of the bitumen and natural gas in this formation.

CONCLUSIONS

Petrological and geochemical studies of exhumed Lower Devonian sandstones and Upper Cambrian siltstones containing bitumen in the Tianjingshan area in the NW Sichuan Basin have allowed the following major conclusions to be drawn:

1. Two different types of bitumen were identified in Palaeozoic reservoir rocks: Lower Devonian soft bitumen and Upper Cambrian solid bitumen, with respective reflectances (BR_o) of 0.26-0.27% and 0.66%.

2. Two types of hydrocarbon inclusions were found in the Lower Devonian sandstones: liquid petroleum and gaseous hydrocarbon inclusions. The two types of bitumen correspond to these two types of inclusions, indicating that two separate oil charge events have occurred.

3. The early-formed oil was generated from Lower Cambrian black shale source rocks in hangingwall kitchens of the Tianjingshan fault, and charged Lower Devonian and Upper Cambrian reservoir rocks during the Early-mid Triassic. The oil was thermally degraded into solid, high maturity bitumen during the Late Triassic.

4. The later oil was sourced from Lower Cambrian black shales in footwall kitchens and charged Lower Devonian reservoir rocks during the Early-mid Jurassic. It was altered into soft low-maturity bitumen

by biodegradation during post-Jurassic uplift of the reservoir rocks.

ACKNOWLEDGEMENTS

This research was supported by National Key Basic Research Programme of China (973 Programme, 2012CB214705), a Special Founding from the State Major Research Programme of China (2011ZX05008-002-40) and the National Natural Science Fund of China (Grant No. 41072095). The authors are grateful to JPG staff for assistance with the English language editing, and to John Parnell (*Aberdeen University*) and Keyu Liu (*CSIRO, Perth*) for reviews which improved the original manuscript significantly. This is Contribution NO. IS-1725 from GIGCAS.

REFERENCES

APLIN, A.C., LARTER, S.R., BIGGE, M.A., MACLEOD, G., SWARBRICK, R.E., GRUNBERGER, D., 2000. PVTX history of the North Sea's Judy oilfield. *Journal of Geochemical Exploration,* **69–70**, 641–644.

BARKER, C., 1990. Calculated volume and pressure changes during the thermal cracking of oil to gas in reservoirs. *AAPG Bulletin*, **74**(8), 1254-1261.

BARON, M., PARNELL, J., MARK, D., CARR, A., PRZYJALGOWSKI, M. and FEELY., M., 2008. Evolution of hydrocarbon migration style in a fractured reservoir deduced from fluid inclusion data, Clair Field, West of Shetland, UK. *Marine and Petroleum Geology*, **25**, 153-172.

BLAMEY, N. J. F., CONLIFFE, C., PARNELL, J., RYDER, A. G. and FEELY, M., 2009. Application of fluorescence lifetime measurements on single petroleum-bearing fluid inclusions to demonstrate multicharge history in petroleum reservoirs. *Geofluids*, **9,** 330-337.

BLANCHET, A., PAGEL, M., WALGENWITZ, F. and LOPEZ, A., 2003. Microspectrofluorimetric and micro-thermometric evidence for variability in hydrocarbon inclusions in quartz overgrowths: implications for inclusion trapping in the Alwyn North field, North Sea. *Organic Geochemistry*, **34**, 1477–1490.

BODNAR, R.J., 1990. Petroleum migration in the Miocene Monterey Formation, California, USA: constraints from fluid inclusion studies. *Mineralogical Magazine*, **54**, 295–304.

BRUNSGAARD, H.S., BERG, R.W. and STENBY, E.H., 2001. High-pressure measuring cell for Raman spectroscopic studies of natural gas. *Applied Spectroscopy*, **55**(1), 55-60.

BRUNSGAARD, H.S., BERG, R.W. and STENBY, E.H., 2002. Raman spectroscopic studies of methane-ethane mixtures as a function of pressure. *Applied Spectroscopy*, **55**(6), 745-749.

CAI, C. F., ZHANG, C. M., CAI, L. L., WU, G. H., JIANG, L., XU, Z. M., LI, K. K., MA, A. L. and CHEN, L. X., 2009a. Origins of Palaeozoic oils in the Tarim Basin: Evidence from sulfur isotopes and biomarkers. *Chemical Geology*, **268**, 197–210.

CAI, C. F., LI, K. K., MA, A. L., ZHANG, C. M., XU, Z. M., WORDEN, R. H., WU, G. H., ZHANG, B. S., and CHEN, L. X., 2009b. Distinguishing Cambrian from Upper Ordovician source rocks: Evidence from sulfur isotopes and biomarkers in the Tarim Basin. *Organic Geochemistry,* **40,** 755–768.

CAI, X.Y., MA, Y.S. and LI, G.X., 2005. The reservoir characteristic of the Feixianguan formation in the lower Triassic in Puguang gas pool. *Journal of Oil and Gas Technology* (J. JPI), **27**(1), 43-45 (in Chinese).

CAI, X.Y., ZHU, Y. M. and HUANG, R.C., 2006. Geochemical behaviours and origin of reservoir bitumen in Puguang gas pool. *Oil & Gas Geology*, **27**(3), 340-347 (in Chinese).

CAI, X. Y. and WANG, Y., 2008. The formation and distribution of the marine hydrocarbon source rock in the Tarim Basin, NW China. *Acta Geologica Sinica*, **82**(3), 509-519.

CHEN, Y., ZHAO, X.F., LIU, S.G. and LIU, C.F., 2009. Transition from marine clastic rocks to non-marine clastic rocks in the west of Sichuan Basin, China. *Journal of Chengdu University of Technology (Science & Technology Edition)*, **36**(6), 697-705 (in Chinese).

CHEN, S.F., DENG, Q.D., ZHAO, X.L., C. J. L. WILSON., P. DIRKS., LUO, Z.L., and LIU, S.G., 1994. Deformational characteristics, evolutionary history, and deformation mechanism of the middle Longmenshan Thrust-Nappes and related tectonics. *Seismology and Geology*, **16** (4), 413-420 (in Chinese)

CHEN, Z.X., JIA, D., WEI, G.Q., LI, B.L., ZENG, Q. and HU, Q.W., 2005. Structural analysis of Kuangshanliang in the northern Longmenshan fold-thrust belt and its hydrocarbon exploration. *Earth Science Frontiers*, **12**(4), 445-450 (in Chinese).

DAI, H.M., LIU, W.L., YANG, Y.M., LI, Y.G. and DUAN, Y., 2007. The origin of Jurassic oil-soaked sandstone in the piedmont zone of north Longmenshan, the Sichuan Basin. *Petroleum Geology & Experiment*, **29**(6), 604-608 (in Chinese).

DENG, H.C., ZHOU, W., QIU, D.Z. and XIE, R.C., 2008. Oil sand-forming conditions and evaluation on resource of oil sand in Tianjingshan Structure in northwest part of Sichuan Basin. *Journal of Jilin University (Earth Science Edition)*, **38**(1), 69-75 (in Chinese).

ECPGC (Editorial Committee of Petroleum Geology of China), 1993. Petroleum Geology of China: Sichuan Oil and Gas Field (Vol. 10), China Petroleum Industry Press, Beijing, pp.1-498(in Chinese).

FABRE, D. and OKSENGORN, B., 1992. Pressure and density dependence of CH_4 and N_2 Raman lines in an equimolar CH_4/N_2 gas mixture [J]. *Applied Spectroscopy*, **46**(3), 468-471.

FEELY, M., and PARNELL, J., 2003. Fluid inclusion studies of well samples from the hydrocarbon prospective porcupine Basin, offshore Ireland. *Journal of Geochemical Exploration*, 78-79, 55-59.

GAO, F., 2009. The distribution and characteristics of paleo-oil reservoirs in China. *Inner Mongolia Petrochemical Industry*, **2**, 108-109.

GEORGE, S. C., RUBLE, T.E., DUTKIEWICZ, A. and EADINGTON, P.J., 2001. Assessing the maturity of oil trapped in fluid inclusions using molecular geochemistry data and visually-determined fluorescence colours. *Applied Geochemistry*, **16**, 451–473.

GROSJEAN, E., LOVE, G. D., STALVIES, C., FIKE, D. A. and SUMMONS, R. E., 2009. Origin of petroleum in the Neoproterozoic–Cambrian South Oman Salt Basin. *Organic Geochemistry*, **40**, 87–110.

GROSJEAN, E., LOVE, G. D., KELLY, A. E., TAYLOR, P. N. and SUMMONS, R. E., 2012. Geochemical evidence for an Early Cambrian origin of the 'Q' oils and some condensates from north Oman. *Organic Geochemistry,* **45**, 77-90.

GRUNDMAN, G., BEHAR, F., MALO, M., BAUDIN, F. and LORANT, F., 2012. Evaluation of hydrocarbon potential of the Paleozoic (Cambrian - Devonian) source rocks of the Gaspé Peninsula, Québec, Canada: Geochemical characterization, expulsion efficiency, and erosion scenario. *AAPG Bulletin*, **96**(4), 729-751.

HAN, S.Q., WANG, S.D. and HU, W.Y., 1982. The discovery of a paleopool in Majiang and its geological significance. *Oil &*

Gas Geology, **3**(4), 316-327.
HAO, F., GUO, T.L., ZHU, Y.M., CAI, X.Y., ZOU, H.Y. and LI, P.P., 2008. Evidence for multiple stages of oil cracking and thermochemical sulfate reduction in the Puguang gas field, Sichuan Basin, China. *AAPG Bulletin*, **92**(5), 611-637.
HAYES, J.M., 1991. Stability of petroleum. *Nature* **352**, 108–109.
HU, A.P., YANG, C., DAI, J.X., MA, Y.S. and GUO, T.L., 2010. Characteristics of reservoir bitumen in Puguang and Maoba gas fields with high H_2S content in north-eastern Sichuan Basin. *Acta Petrolei Sinica*, **31**(2), 231-236 (in Chinese).
HUANG, D.F. and WANG, L.S., 2008. Geochemical characteristics of bituminous dike in Kuangshanliang area of the Northwestern Sichuan Basin and its significance. *Acta Petrolei Sinica*, **29**(1), 23-28 (in Chinese).
HUANG, J.L., ZOU, C.N., LI, J.Z., DONG, D.Z., WANG, S.J., WANG, S.Q. and CHENG, K.M., 2012. Shale gas generation and potential of the Lower Cambrian Qiongzhusi Formation in the Southern Sichuan Basin, China. *Petrol. Explor. Develop*., **39**(1), 75–81.
HUANG, W.M., LIU, S.G., XU, G.S., WANG, G.Z., MA, W.X., ZHANG, C.J. and SONG, G.Y., 2011. Characteristics of paleo oil pools from Sinian to Lower Paleozoic in southeastern margin of Sichuan Basin. *Geological Review*, **57**(2), 285-299.
HUANG, X.M. and XIE, F. R., 2009. Review of the evolutionary history and tectonic style of the Longmenshan Tectonic Belt. *Corpus of Crustal Structure and Stress*, **21**, 16-29 (in Chinese).
JIA, D., WEI, G.Q., CHEN, Z.X., LI, B.L., ZENG, Q. and YANG, G., 2006. Longmen Shan fold-thrust belt and its relation to the western Sichuan Basin in central China: New insights from hydrocarbon exploration. *AAPG Bulletin*, **90(**9), 1425-1447.
JONK, R., PARNELL, J. and WHITHAN, A., 2005. Fluid inclusion evidence for a Cretaceous-Palaeogene petroleum system, Kangeilussuaq Basin, East Greenland. *Marine and Petroleum Geology*, **22**, 319-330.
LI, J., LI, Z. Q., WANG, P., 2012. The preliminary analysis of structure pattern of Longmeshan tectonic zone of Sichuan. *Yunan Geology*, **31**(2), 272-276 (in Chinese).
LI, R.W., LU, J.L., ZHANG, S.K. and LEI, J.J., 1999. Organic carbon isotopes of the Sinian and Early Cambrian black shales on Yangtze Platform, China. *Science in China, Series D,* **29**(4), 351-357 (in Chinese).
LI, Y., ZHOU Y.Q., YAN, S.Y. and YANG H.S., 2008. Establishment of tectonic evolution pattern of Long menshan Orogen. *Journal of China University of Petroleum* **32**(2), 12-15.
LIN, J.S., XIE, Y., LIU, J.Q., ZHAO, Z., JING, X.Y. and CHENG, H., 2011. Restudy of the Source Rock of Majiang Paleo-Reservoir. *Geological Science and Technology Information,* **30**(6), 105-109.
LIU, C., ZHANG, H.L., SHEN, A.J., QIAO, Z.F., NI, X.F. and ZHAO, X.Q., 2010. Geochemistry characteristics and origin of the Devonian oil-sandstone in the northwest of Sichuan Basin. *Acta Petrolei Sinica*, **31**(2), 253-258 (in Chinese).
LIU, D.H., DAI, J.X., XIAO, X.M., TIAN, H., YANG, C., HU, A.P., MI, J.K. and SONG, Z.G., 2010. High density methane inclusions in Puguang gasfield: Discovery and a T-P genetic study. *Chinese Science Bulletin,* **54**, 4714-4723.
LIU, D.H., XIAO, X.M., MI, J.K., LI, X.Q., SHEN, J.K., SONG, Z.G. and PENG, P.A., 2003. Determination of trapping pressure and temperature of petroleum inclusions using PVT simulation software – a case study of Lower Ordovician carbonates from the Lunnan Low Uplift, Tarim Basin. *Marine and Petroleum Geology*, **20**, 29–43.
LIU, D.M., TU, J.Q. and JIN, K.L., 2003. Organic petrology of potential source rocks in the Tarim Basin, NW China. *Journal of Petroleum Geology*, **26**(1), 105-124.
LIU, G.X., WANG, S.D., PAN, W.L. and LV, J.X., 2003. Characteristics of Tianjingshan destroyed oil reservoir in Guangyuan area, Sichuan. *Marine Origin Petroleum Geology*, **8** (1-2), 103-108 (in Chinese).
LIU, S.G., MA, Y.S., SUN, W., CAI, X.Y., LIU, S., HUANG, W.M. and XU, G.S., 2008. Studying the differences of Sinian natural gas pool between Weiyuan gas field and Ziyang gas-prone area, Sichuan Basin. *Acta Petrolei Sinica*, **82**(3), 328-337 (in Chinese).
LIU, S.G., MA, Y.S., CAI, X.Y., XU, G.S., WANG, G.Z., YONG, Z.Q., SUN, W., YUAN, H.F. and PAN, C.L., 2009. Characteristic and accumulation process of the natural gas from Sinian to Lower Paleozoic in Sichuan Basin, China. *Acta Geologica Sinica*, **36**(4), 345-354.
LIU, S.G., YANG, R.J., WU, X.C., SUN, W. and CHEN, Y., 2009. The Late Triassic transition from marine carbonate rock to clastics in the western Sichuan Basin. *Oil & Gas Geology,* **30**(5), 556-565. (in Chinese).
LIU, S.H., HU, W.Y., QIU, Y.X. and CHEN, Y.B., 1985. Discussion on the Oil Source and Diagenetic Sequence of the Wongxiang Group in Fossil Majiang Pool. *Oil & Gas Geology,* **6**(2), 127-140.
MACHEL, H.G., KROUSE, H.R. and SASSEN, R., 1995. Products and distinguishing criteria of bacterial and thermochemical sulfate reduction [J]. *Applied Geochemistry*, **10**(4), 373 – 389.
MA, Y.S., CAI, X.Y. and LI, G.X., 2005. Basic characteristics and concentration of the Puguang gas field in the Sichuan Basin. *Acta Geology Sinica*, **79**(6), 858-865 (in Chinese).
MA, Y.S., GUO, X.S. and GUO, T.L., 2005. Discovery of the large-scale Puguang gas field in the Sichuan Basin and its enlightenment for hydrocarbon prospecting. *Geological Review,* **51**(4), 477-480 (in Chinese).
MA, Y.S., ZHANG, S.C., GUO, T.L., ZHU, G.Y., CAI, X.Y. and LI, M.W., 2008. Petroleum geology of the Puguang sour gas field in the Sichuan Basin, SW China. *Marine and Petroleum Geology*, **25**, 357–370.
McLIMANS, R.K., 1987. The application of ûuid inclusions to migration of oil and diagenesis in petroleum reservoirs. *Applied Geochemistry*, **2**, 585–603.
MI, J.K., XIAO, X.M., LIU, D.H. and SHEN, J.K., 2004. Determination of paleo-pressure for a natural gas pool formation based on PVT characteristics of fluid inclusions in reservoir rocks - A case study of Upper-Paleozoic deep basin gas trap of the Ordos Basin. *Science in China Ser. D Earth Sciences,* **47**(6), 507-513.
NIU, H.L., XIE, R.C., ZHAO, A.K. and JIN, W.H., 2011. Characteristics and main controlling factors of reservoirs of Silurian paleopool in Majiang. *Petroleum Geology and Engineering,* **25**(4), 32-35.
PANG, Y.J., ZHANG, B.J., FENG, R.W., and WANG, Y.R., 2010. Evolution of Devonian depositional environment in northern Longmenshan tectonic belt. *Global Geology*, **29**(4), 561-568 (in Chinese).
PARNELL, J., CAREY, P. and DUNCAN, W., 1998. History of hydrocarbon charge on the Atlantic margin: Evidence from fluid-inclusion studies, West of Shetland. *Geology*, **26**, 807-810.
PARNELL, J., MIDDLETON, D., CHEN, H.H. and HALL, D., 2001. The use of integrated fluid inclusions studies in constraining oil charge history and reservoir compartmentation: examples from the Jeanne d'Arc Basin, offshore Newfoundland. *Marine and Petroleum Geology*, **18**, 535–549.
PARFENOVA, T.M., KONTOROVICH, A.E., BORISOVA, L.S. and MELENEVSKII, V.N., 2010. Kerogen from the Cambrian deposits of the Kuonamka Formation (northeastern Siberian Platform). *Russian Geology and Geophysics*, **51**, 277–

285.

PEPPER, A. S. and DODD, T. A., 1995. Simple kinetic models of petroleum formation. Part II: oil-gas cracking. *Marine and Petroleum Geology*, **12**(3), 321-340.

QIN, J.Z., FU, X.D. and LIU, X.Z., 2007. Solid bitumens in the marine carbonate reservoir of gas field in the Northeast Area of the Sichuan Basin. *Acta Geologica Sinica*, **81**(8), 1065-1071.

QIN, J.Z., FU, X.D. and TENG, G.E., 2008. Evaluation of the excellent Triassic to Silurian marine hydrocarbon source rocks in Xuanhan-Daxian area of Northeast Sichuan Basin. *Petroleum Geology & Experiment*, **30**(4), 367-375 (in Chinese).

QU, D.C., 2004. Development tracing analyses of Leisan gas reservoir in Zhongba. *Natural Gas Exploration & Development*, **27**(1), 30-32.

RAO, D., QIN, J.Z., TENG, G.E. and ZHANG, M.Z., 2008. Source analysis of oil seepage and bitumen originating from marine layer strata in Guangyuan area, the northwest Sichuan Basin. *Petroleum Geology and Experiment*, **30**(6), 596-605 (in Chinese).

SCHENK, H. J., DI PRIMIO, R. and HORSFIELD, B., 1997. The conversion of oil into gas in petroleum reservoirs. Part I: Comparative kinetic investigation of gas generation from crude oils of lacustrine, marine and fluvio-deltaic origin by programmed-temperature closed-system pyrolysis. *Organic Geochemistry*, **26**(7-8), 467-481.

STASIUK, L.D. and SNOWDON, L.R., 1997. Fluorescence micro-spectrometry of synthetic and natural hydrocarbon fluid inclusions: crude oil chemistry, density, application to petroleum migration. *Applied Geochemistry*, **12**, 229–241.

SUN, W., LIU, S.G., MA, Y.S., CAI, X.Y., XU, G.S., WANG, G.Z., YONG, Z.Q., YUAN, H.F. and PAN, C.L., 2007. Determination and Quantitative Simulation of Gas Pool Formation Process of Sinian Cracked Gas in Weiyuan - Ziyang Area, Sichuan Basin. *Acta Geologica Sinica,* **81**(8), 1153-1159.

SUN, X.M., XU, Q.W., WANG, Y.D., TIAN, J.X., WANG, S.Q. and DU, J.Y., 2010. Reservoir forming characteristics and main controlling factors of oil sandstones in the northern Longmen Mountain thrust zone of the Northwest of Sichuan. *Journal of Jilin University (Earth Science Edition)*, **40**(4), 886-896 (in Chinese).

SWEENEY, J. J. and BURNHAM, A. K., 1990. Evaluation of a simple model of vitrinite reflectance based on chemical kinetics. *AAPG Bull.*, **74**, 1559-1570.

TENG, G.E., QIN, J.Z., FU, X.D., LI, W., RAO, D. and ZHANG, M.Z., 2008. Basic conditions of marine hydrocarbon accumulation in northwest Sichuan Basin-high quality source rocks. *Petroleum Geology & Experiment*, **30**(5), 478-483 (in Chinese).

TIAN, H., XIAO, X.M., WILKINS, R.W.T., GAN, H.J., XIAO, Z.Y., LIU, D.H. and GUO, L. G., 2008. Formation and evolution of Silurian paleo-oil pools in the Tarim Basin, NW China. *Organic Geochemistry*, **39**, 1281–1293.

TONG, C.G. and HU, S.Q., 1997. Prospective value of oil and gas in the foothill belt of the North Longmen Mountains. *Journal of Chengdu University of Technology,* **24**(2), 1-8

WANG, L.S., HAN, K.Q., XIE, B.H., ZHANG, J., DU, M., WAN, M.X. and LI, D., 2005. Reservoiring conditions of the oil and gas fields in the north section of Longmen Mountain nappe structural belts. *Natural Gas Industry*, **25**, 1-5 (in Chinese).

WANG, Y.P., WANG, Z.Y., ZHAO, C.Y., WANG, H.J., LIU, J.Z. and LIU, D.H., 2007. Kinetics of hydrocarbon gas generation from marine kerogen and oil: Implications for the origin of natural gases in the Hetianhe gasfield, Tarim, NW China. *Journal of Petroleum Geology,* **30**(4), 339-356.

WANG, S.D., ZHENG, B. and CAI, L.G., 1997. The destroyed oil pools in South China and hydrocarbon prospecting. *Marine Origin Petroleum Geology*, **2(**1), 44-50.

WANG, T.S., GENG, A.S., SUN, Y.G., XIONG, Y.Q., LIU, D.H. and LI, X., 2008. Geochemical characteristics of solid bitumen in reservoir and their implication for the origin of natural gas of Feixianguan Formation in Northeastern Sichuan Basin. *Acta Sedmentologica Sinica*, **26**(2), 340-348.

WANG, Y.F. and XIAO, X.M., 2010. An investigation of paleogeothermal gradients in the northeastern part of Sichuan Basin. *Marine Origin Petroleum Geology*, **15**(4), 57-61 (in Chinese).

XIANG, C.F., TANG, L.J., JIN, Z.J., LI, R.F., WANG, P.W. and DONG, L., 2008. Outcrop sequence stratigraphy of the Majiang Ancient Oil Reservoir and its suggestion to the study on the sealing capability of the marine oil field developed in South China. *Acta Geologica Sinica*, **82**(3), 346-352.

XIAO, X.M., LIU, Z.F., MI, J.K., LIU, D.H., SHEN, J.K. and SONG, Z.G., 2002. Dating formation of natural gas pools using fluid inclusions data from reservoirs. *Chinese Science Bulletin*, **47**(8), 1567-1572.

XIAO, X.M., HU, Z.L., JIN, Y.B. and SONG, Z.G., 2005. Hydrocarbon source rocks and generation history in the Lunnan oilfield area, northern Tarim Basin (NW China). *Journal of Petroleum Geology*, **28**(3), 319-333.

XIAO, X.M., ZENG, Q.H., TIAN, H., WILKINS, R.W.T. and TANG, Y.C., 2005. Origin and accumulation model of the AK-1 natural gas pool from the Tarim Basin, China. *Organic Geochemistry,* **36**, 1285–1298.

XIAO, X.M., WANG, F., WILKINS, R.W.T., SONG, Z.G., 2007. Origin and gas potential of pyrobitumen in the Upper Proterozoic strata from the Middle Paleo-Upper of the Sichuan Basin, China. *International Journal of Coal Geology,* **70,** 264-276

XIAO, X. M., TIAN, H., LIU, D. H., LIU, Z. F., 2012. Evaluation of deep burial source rocks and their natural gas potentials in Sichuan Basin. Annual Report of State Major Research Program of China (Project No. 2011ZX05008-002-40), *Internal Report,* Guangzhou Institute of Geochemistry of Chinese Academy of Sciences, pp.1-68 (in Chinese).

XIE, B.H., WANG, L.S., ZHANG, J. and CHEN, S.J., 2003. Vertical distribution and geochemical behaviours of the hydrocarbon source rocks in the north section of Longmen Mountains. *Natural Gas Industry*, **23**(5), 21-23 (in Chinese).

XIE, Z.Y., TIAN, S.C., WEI, G.Q., LI, J., ZHANG, L. and YANG, W., 2005. The study on bitumen and foregone pool of Feixianguan oolitic, northeast Sichuan Basin. *Natural Gas Geoscience*, **16**(3), 283-288.

XU, S.Q., ZENG, Q., TANG, D.H. and ZHANG, G.R., 2005. Analysis on reservoir forming conditions of Houba oil sands in Jiangyou area. *Natural Gas Exploration & Development*, **28**(3), 1-4 (in Chinese).

YANG, C.Q., YUE, Q.L., YAN, J.H. and YU, F.S., 2010. Tectonic deformation features and physical modeling of northern section of Longmenshan mountains. *Fault – Block Oil & Gas Field*, **17**(6), 686-689 (in Chinese).

ZENG, D.M., WANG, X.Z., SHI, X., ZHANG, F., WANG, J. and ZHU, Y.G., 2010. Characteristic and reservoir property of the Leikoupo Formation of Middle Triassic in Northwestern Sichuan Basin. *Acta Sedimentologica Sinica*, **28**(1), 42-49.

ZHANG, L., WEI, G.Q., HAN, L., WANG, L.L. and WANG, D.L., 2008. Evaluation of the high and over matured Sinian-Lower Palaeozoic source rocks in the Sichuan Basin. *Petroleum Geology & Experiment*, **30**(3), 287-291 (in Chinese).

ZHANG, L., WEI, G.Q., WU, S.X., WANG, Z.C., XIAO, X.M., ZHANG, P.J. and SHEN, Y.H., 2005. Distribution characters and hydrocarbon – generating potential of bitumen of

Sinian – Lower Paleozoic in Sichuan Basin. *Petroleum Geology & Experiment,* **27**(3), 276-280.

ZHANG, S.C., HANSON, A.D., MOLDOWAN, J.M., GRAHAM, S.A., LIANG, D.G., CHANG, E., 2000. Paleozoic oil-source rock correlations in the Tarim basin, NW China. *Organic Geochemistry*, **31**, 273-286.

ZHANG, S.C. and ZHU, G.Y., 2006. Gas accumulation characteristics and exploration potential of marine sediments in Sichuan Basin [J]. *Acta Petrolei Sinica*, **27**(5), 1-8 (in Chinese).

ZHAO, W.Z., LUO, P., CHEN, G.S., CAO, H. and ZHANG, B.M., 2005. Origin and reservoir rock characteristics of dolostones in the Early Triassic Feixianguan Formation, NE Sichuan Basin, China: Significance for future gas exploration. *Journal of Petroleum Geology*, **28**(1), 83-100.

ZHAO, W.Z., WANG, Z.C. and WANG, Y.G., 2006. Formation mechanism of highly effective gas pools in the Feixianguan Formation in the NE Sichuan Basin. *Geological Review*, **57**(2), 708-719.

ZHAO, X.Q., CHEN, J.F., ZHANG, T.L., LIU, Y., WU, X.F., LIU, Y.Z. and LIU, F.F., 2012. Geochemical characteristics and genesis of reservoir bitumen of Feixianguan Formation in Well Puguang-2, Northeast of Sichuan. *Acta Sedmentologica Sinica,* **30**(2), 375-384.

ZHOU, W., DENG, H.C., QIU, D.Z. and XIE, R.C., 2007. The discovery and significance of the Devonian paleo-reservoir in Tianjingshan structure of the Northwest Sichuan, China. *Journal of Chengdu University of Technology (Science & Technology Edition)*, **34**(4), 413-417 (in Chinese).

ZHU, G.Y., DAI, J. X. and ZHANG, S. C., LI, J., SHI, D. and WEN, Z. G., 2004. Generation mechanism and distribution characteristics of hydrogen sulfide bearing gas in China [J]. *Natural Gas Geoscience*, **15**(2), 166-170 (in Chinese).